PFC/JA-88-37

RF Assisted Ohmic Current Ramp Up in the Compact Ignition Tokamak

Bonoli, P. T., Porkolab, M.

Plasma Fusion Center
Massachusetts Institute of Technology
Cambridge, MA 02139

January 1989

This work was supported by the U. S. Department of Energy Contract No. DE-AC02-78ET51013. Reproduction, translation, publication, use and disposal, in whole or in part by or for the United States government is permitted.

RF Assisted Ohmic Current Ramp Up in the Compact Ignition Tokamak

P. T. Bonoli and M. Porkolab
MIT
Cambridge, MA 02139
USA

Abstract

A simulation model for lower hybrid current drive (LHCD) has been used to study RF assisted ohmic current ramp up in the Compact Ignition Tokamak (CIT). The low electron density, high toroidal magnetic field, and positive DC electric field present during the ohmic current ramp up phase of CIT make LHRF current drive an excellent candidate for doing RF assist during current ramp up. Typical LHRF currents (I_{rf}) of the order of $I_{rf} \lesssim I_p$ can be expected, resulting in a (25-35)% increase in the current ramp rate.

I. Introduction

Recently, RF current ramp up and transformer recharging have been demonstrated in toroidal devices using lower hybrid (LH) RF current generation /1-4/. These experiments were performed with and without the ohmic heating (OH) transformer turned on. Possible benefits to be gained from ramping the total plasma current with OH plus RF drive would be a savings in the volt-second requirments of the OH transformer and/or the achievement of the same total current as with OH ramp alone, but in a shorter time.

The electron densities ($n_{eo} \lesssim 1 \times 10^{20}\mathrm{m}^{-3}$) and toroidal magnetic fields ($7 \leq B_\phi \leq$ 10T) envisioned for the current ramp up phase of the Compact Ignition Tokamak (CIT) /5/ are particularly well suited for highly efficient RF current generation using injected LH waves. In addition, the presence of the DC electric field should further enhance the RF current generation because of an increase in the electron tail population in the direction of the electric field drift, i.e., the direction of current drive. For the model results presented in this LETTER, values of the current drive figure of merit of $\eta_{cd} \gtrsim 0.35$ A/W/m^2 were found. Here $\eta_{cd} = \bar{n}_e\ (10^{20}\mathrm{m}^{-3})\ I_{rf}\ (\mathrm{MA})\ R_o(\mathrm{m})/P_{LH}\ (\mathrm{MW})$, where $\bar{n}_e$ is the line average electron density, I_{rf} is the net RF current, and P_{LH} is the injected LHRF power. For P_{LH} = 10 MW, R_o = 2.1 m, and $\bar{n}_e = 3 \times 10^{19}\mathrm{m}^{-3}$, we predict $I_{rf} \simeq 5.35$ MA in 8 seconds, so that I_{rf} is comparable to I_p and significant total current ramp up would be expected. An important result of the numerical studies is that a significant fraction of the rise in total plasma current during OH plus RF ramp is due to the effect of ohmic plasma heating alone. This can be understood by recalling that $J_{\|} \propto T_e^{3/2}$ for an assumed plasma model of Spitzer resistivity (where $J_{\|}$ is the total plasma current density along $\underline{B}_o$). For the CIT relevant case discussed here, the current ramp rate was found to be 0.74 MA/sec. with OH ramp alone and 1.05 MA/sec. with OH plus RF ramp. As a result, it was possible to ramp I_p from 1.0 MA to 9.64 MA with OH plus RF, which should be compared to 7.3 MA with OH alone.

The plan of this paper is as follows. In Sec. II a brief description of the simulation model for LHCD is given. The results of the numerical modelling are presented and discussed in Sec. III and the conclusions are given in Sec. IV.

II. Description of Model

The simulation model used in the numerical studies has been described in detail in Refs. /6/ and /7/. Briefly, the model incorporates a 1-D radial transport code, a parallel velocity Fokker Planck calculation, and a toroidal ray tracing code. An evolution equation for the poloidal flux function $\psi(r,t)$ is solved in conjunction with Maxwell's equations and the transport equations. The electron thermal diffusivity is taken to be that due to Tang for the ohmic plasma and $\chi_e^{RF} = M_e \chi_e^{TANG}$ in the presence of RF injection. $M_e \geq 1$ is adjusted to achieve the desired electron temperature /7/. The Fokker Planck calculation is relativistically correct and includes the effects of the DC electric field and an arbitrary perpendicular (velocity) electron temperature due to pitch angle scattering of electrons. The toroidal ray tracing utilizes a Shafranov representation for the magnetic field $\underline{B}$ and includes multiple radial reflections of the LH ray trajectories. Finally, the quasilinear RF diffusion coefficient used in the Fokker Planck analysis is a self-consistent function of the local wave damping /6/.

III. Simulation Results

The parameters used in the simulation of LHRF assisted current ramp up in CIT were $n_{eo} = 5 \times 10^{19}$ m^{-3}, $n_{eo} = 1.5 \times \overline{n}_e$, $n_{ea} = 0.1 \times n_{eo}$, $B_\phi = 8$T, deuterium plasma, $a = 0.7$m, $R_o = 2.1$ m, $I_p = 1$ MA (initially), $Z_{eff} = 1.5$, $f_o = 10$ GHz, and $P_{LH} = 10$ MW. In these simulations, the electron density and the toroidal magnetic field are kept constant as a function of time. However, the voltage impressed by the primary circuit of the OH transformer ($V_{OH}(t)$) is raised to $V_{OH} = 5.5V$ as the RF is turned on and maintained at that value for the duration of the RF pulse (Δt_{RF} = 8.25 sec.). The multiplier on the electron thermal diffusivity was chosen to be $M_e = 4.5$ so that a final value of $T_{eo} \simeq 8$ keV was obtained during RF injection. It is important to point out that too large an electron temperature increase during current ramp up is undesirable because the plasma current diffusion time ($\tau_{L/R}$) will become too long, making it more difficult to change the total plasma current in a prescribed time. In the results shown below, it will be seen that the deleterious effects of an increased L/R time during current ramp up are offset to some extent by the generation of RF current at $r/a \approx 0.5$ where T_e is lower ($\sim$ 5 keV).

The LH wave accessibility is excellent for these parameters with $\omega_{pe}/\omega_{ce} = 0.28$ and $n_{\|acc} = 1.32$ /8/. Here $n_{\|} = k_{\|}c/\omega$ is the parallel refractive index of the injected LH waves and $n_{\|acc}$ is the minimum value of $n_{\|}$ accessible to the plasma center.

The choice of RF frequency (10 GHz) was motivated by the consideration that if LHRF were to be used during the initial current ramp up phase of CIT, then it would be desirable to use this RF source for bulk electron heating and/or current profile control during the deuterium-tritium (D-T) burn phase of the discharge ($n_{eo} \gtrsim 5 \times 10^{20}$ m^{-3} and $T_{eo} \sim T_{io} \gtrsim$ 15 keV). In order to avoid parametric decay of the injected LH waves /9/ it is necessary to keep $\omega/\omega_{LH}(0) > 2$, which is easily satisfied for f_o = 10 GHz, B_ϕ = 10T, and $n_{eo} = 6 \times 10^{20}$ m^{-3}. Also, during the burn phase of CIT a population of fusion generated alpha particles would be present. In order to avoid absorption of the injected LH waves on the alpha particles one must choose f_o so that the LH waves cannot resonate with fusion alpha particles whose energies are below the alpha birth energy (E_o = 3.5 MeV). This greatly reduces the Landau absorption of LH waves on energetic alpha particles because the alpha particle density is small at energies $E_\alpha > E_o$. The condition $E_\alpha = \frac{1}{2}m_\alpha(\omega/k)^2_{LH} > E_o$ can be written using the electrostatic LH dispersion relation as $f_o \gtrsim 0.29\, \omega_{LH}(0) n_{\|}(Z^*)^{1/2}$, where $Z^* = (\Sigma n_i m_p Z_i^2/n_e m_i)^{-1}$, m_p is the proton mass, and the sum is over deuterium and tritium ions. For edge current profile control at $n_e \simeq 2 \times 10^{20}$ m^{-3}, B_ϕ = 10T, and 50/50 D-T plasma, one calculates $n_{\|acc} \simeq 1.5$ and $f_o \gtrsim$ 6.5 GHz. Nevertheless, the results shown below have also been reproduced with f_o = 4.6 GHz.

The injected RF power spectrum was assumed to have the form

$$S(n_{\|}) = \exp[-(n_{\|} - \bar{n}_{\|})^2/(\Delta n_{\|}^o)^2], \; n_{\|} > 0 \quad , \qquad 1(a)$$

$$S(n_{\|}) = 0 \qquad\qquad n_{\|} < 0 \quad , \qquad 1(b)$$

where $\bar{n}_{\|} = 1.75$ and $\Delta n_{\|}^o = 0.25$.

A. Model Results for LHRF Assisted Ramp Up

The results of the OH plus RF current ramping are shown in Figs. 1-3. The radial profiles of RF power absorption (S_{rf}) and RF current generation (J_{rf}) are shown in Figs. 1(a) and 1(b). Although S_{rf} and J_{rf} are rather broad at the later times shown in Fig. 1, the initial profiles (immediately after the RF turn-on) were peaked nearer to $r/a \approx 0.5$. The power absorbed due to resonant electron Landau damping is 9.95 MW with 0.01 MW of RF power absorbed at the plasma periphery due to collisional damping. The power lost due to finite electron tail confinement was negligible (0.11 MW). The corresponding RF current generation was significant with $I_{rf} = 5.35$ MA which gives $\eta_{CD} = 0.38$ A/W/m^2. An enhancement in J_{rf} due to the DC electric field would be expected since $E_{\|}(r) > 0$ everywhere in the plasma (see Fig. 1(c)). Note that although $E_{\|}(r) > 0$, the total plasma current (i.e., $B_\theta(a,t)$) is increasing because of the impressed voltage ($V_{OH} = 5.5V$) of the OH transformer at the plasma edge. Recall from Ref. /7/ that $E_{\|}(a,t)$, V_{OH}, and I_p are related to each other at $r = a$ by

$$2\pi R_o E_{\|}(a,t) = V_{OH}(t) - L_{ext} dI_p/dt \quad . \tag{2}$$

I_p will continue to rise until $V_{\|}(a,t) = 5.5V$. This is to be distinguished from the case of pure RF current ramp where $V_{OH}(t) = 0$ and $E_{\|} < 0$ are the usual conditions for ramping I_p. The electron temperature profiles for the ohmic and RF plasmas are shown in Fig. 1(d). The corresponding ion temperature increased from 1.86 keV to 6.98 keV during RF injection, and the energy content of the plasma increased from 0.20 MJ to 0.84 MJ. The energy confinement time of the discharge decreased from $\tau_E^{OH} = 234$ ms to $\tau_E^{RF} = 43$ ms for the choice of $M_e = 4.5$ in χ_e^{rf}.

The time evolution of I_p and V_L are shown in Figs. 2(a) and 2(b). For comparison, the result of $I_p(t)$ with OH ramp alone is also shown in Fig. 2(a). The case with pure OH ramp was obtained by setting $V_{OH} = 5.5V$ at $t = 0.5$ sec. and not turning the LHRF current drive on at that time. The electron thermal diffusivity in this case was adjusted so that the increase in $T_e(r)$ was the same as in the case with RF drive. The current ramped to 9.64 MA in 8.25 sec. with OH plus RF drive as compared to 7.3 MA with OH ramp alone. The current ramp rates were $\dot{I}_p = 1.05$ MA/sec. and 0.74 MA/sec. for the cases with and without LHRF injection. Thus, the incremental increase in the ramp rate due to the LHRF is approximately $\Delta\dot{I}_p \simeq 0.31$ MA/sec. The time evolution of $V_{\|}(a,t) \equiv V_L$ in Fig. 2(b) indicates that $V_L \simeq 2.65V < V_{OH}$ so that I_p would continue to increase if the discharge was allowed to evolve.

The electron distribution function for $n_{\|} > 0$ and $n_{\|} < 0$ is shown in Fig. 3 and corresponds to a radial location of $r = 19.25$ cm, which is near the maximum of the RF power deposition profile (Fig. 1(a)). The tendency of the DC electric field to enhance the electron distribution function above its Maxwellian value (for $n_{\|} > 0$) is apparent from Fig. 3. The upper limit of the quasilinear plateau ($E \simeq 110$ keV) is in good agreement with the characteristic $n_{\|} = 1.75$ of the injected RF waves. The lower limit of the plateau ($E \simeq 34$ keV) corresponds to $v_{\|}/v_e \approx 2.2$ since $T_e \simeq 6.8$ keV at this radial location. This is consistent with the quasilinear limit for strong electron Landau damping of $v_{\|}/v_e \lesssim 2.4$, where $v_e^2 = 2T_e/m_e$.

B. Model Results for ECRF Assisted Current Ramp Up

A possible OH plus RF assisted current ramp up scenario was also investigated using electron cyclotron (EC) RF current drive. In order to compare with the LHRF results of the previous subsection the following parameters were chosen: $n_{eo} = 5 \times 10^{19}$ m^{-3}, $P_{EC} =$ 10 MW, $B_\phi = 8$T, $a = 0.7$ m, $R_o = 2.1$ m, $I_p = 1.0$ MA (initially), and $I_{rf} = 0.85$ MA. The value of I_{rf} that was chosen was obtained from the Livermore TORCH ray-tracing/current drive code /10/ and the current drive efficiency of 0.085 Amp/Watt was obtained for $T_e =$ 10 keV. The voltage impressed by the OH transformer (V_{OH}) was programmed so that V_{OH} remained at its pre-RF value during the current ramp up phase. Thus, in this example, the direct effect of the RF current drive on the current ramp rate could be studied, independent of the OH transformer drive. For this case, the total current ramped from $I_p = 1$ MA to 1.65 MA in 6.4 sec., for a ramp rate of 0.1 MA/sec. This ramp rate is considerably smaller than the incremental increase in the ramp rate due to the LHRF ($\Delta \dot{I}_p \simeq 0.31$ MA/sec.). We have also examined other optimized cases at $n_e(0) = 3 \times 10^{19}$ m^{-3}, $T_e(0) = 5$ keV, B_ϕ = 9.2T, and $n_e(0) = 1.0 \times 10^{20}$ m^{-3}, $B_\phi = 7.7$T, $T_e(0) = 10$ keV, and the results obtained for ramping were comparable, or less favorable, to the case discussed above. The reason for the larger effect on $\dot{I}_p$ due to the LHRF drive is the significantly larger LHRF current driven ($I_{rf} = 5.5$ MA) relative to the ECRF current drive case ($I_{rf} \lesssim 1.0$ MA).

IV. Conclusions

The results presented in the previous section indicate that LHRF assisted ramping of the OH current in a tokamak can result in significant savings on the volt-second requirements of the OH transformer. In the case of ECRF, the effects of DC electric field was not included in the current drive efficiency, hence the present result may underestimate the ultimate ramp-up efficiency obtainable by ECH (of the order of 30% in the present simulations of CIT). Thus, the theory of ECR current drive must be developed, including DC electric fields. The relatively high toroidal magnetic fields, low electron densities, and the presence of a positive DC electric field in the plasma during the current ramp up phase of CIT make LHRF injection an excellent candidate for doing the RF assist. Comparisons of OH current ramp with LHRF assisted current drive and ECRF assist indicate that the significant levels of LHRF current generation (relative to ECRF current generation) result in much larger increases in the ramp rate with LHRF.

In order to better assess the feasibility of an OH plus RF assist ramp up scenario two important modifications need to be made in the simulation results presented. First the electron density and toroidal magnetic field should be ramped simultaneously with the current /5/, and second, the wave propagation and absorption should be recalculated in the non-circular geometry characteristic of CIT plasmas. Such calculations will be carried out in the future. Nonetheless, the model calculations presented in this LETTER do demonstrate the possibility of achieving a significant increase in the rate of OH current ramp using LHRF injection, and possibly ECRF if the current drive efficiency could be improved by the DC electric field.

Acknowledgements

We wish to thank D. Ignat, B. Montgomery, and R. Parker for drawing our attention to this problem of interest for CIT. One of us (M. P.) wishes to thank Kyoko Matsuda of General Atomics, La Jolla, CA, for providing the ECR current drive efficiency data using TORCH code simulations. This work was supported by the U.S. Department of Energy Contract No. DE-AC02-78ET51013.

References

/1/ Jobes, F. C., Bernabei, S., Chu, T. K., Hooke, W. M., Meservey, E. B., Motley, R. W., Stevens, J. E., Von Goeler, S., *Phys. Rev. Lett.,* **55** (1985) 1295.

/2/ Porkolab, M., Lloyd, B., Schuss, J. J., Takase, Y., Texter, S., et al., in Heating in Toroidal Plasmas, Proceedings of the 4^{th} International Symposium, Rome, Italy, 1984 (Int. School of Plasma Phys., Varenna, 1984), Vol. I, p. 529.

/3/ Takase, Y., Knowlton, S. F., Porkolab, M., *Phys. Fluids,* **30** (1987) 1169.

/4/ Leuterer, F., Eckhartt, D., Söldner, F., Becker, G., Bernhardi, K., et al., *Phys. Rev. Lett.*, **55** (1985) 75.

/5/ Bateman, G., CIT Conceptual Design Review, (Princeton Plasma Physics Laboratory, Jan., 1988) Publication No. AA-880119-PPL-02.

/6/ Bonoli, P. T., and Englade, R., *Phys. Fluids,* **29** (1986) 2937.

/7/ Bonoli, P. T., Porkolab, M., Takase, Y., Knowlton, S. F., *Nucl. Fusion,* **28** (1988) 991.

/8/ Porkolab, M., in Fusion (Teller, E., ed.), Vol. 1B, Ch. 13, Academic Press, New York (1981) 151.

/9/ Porkolab, M., *Phys. Fluids,* **20** (1977) 2058.

/10/ This value of I_{RF} was obtained by K. Matsuda, General Atomics, using the LLNL TORCH ray tracing code with a current drive package included.

Torch has been developed by A. Kritz and G. Smith [*Bull. Am. Phys. Soc.,* **31** (1986) 1516].

Figure Captions

Fig. 1. OH plus LHRF current ramp-up ($n_{eo} = 5 \times 10^{19}$ m^{-3}, $B_\phi = 8$T, $P_{LH} = 10$ MW, $a =$ 0.7 m, $R_o = 2.1$ m, $f_o = 10$ GHz). (a) Radial profile of RF power density. (b) Radial profile of RF current density. (c) Radial profiles of parallel DC electric field. (d) Radial profiles of electron temperature. Curves labelled OH refer to the ohmic plasma, and all other curves correspond to a time of 8.0 sec. after RF is turned on ($T_{rf} = 0.5$ sec.).

Fig. 2. OH plus LHRF current ramp up for CIT parameters ($n_{eo} = 5 \times 10^{19}$ m^{-3}, $B_\phi =$ 8T, $P_{LH} = 10$ MW, $a = 0.7$ m, $R_o = 2.1$ m, $f_o = 10$ GHz). (a) Time evolution of total plasma current (ohmic plus RF). Shown for comparison is the pure OH ramp case. (b) Time evolution of loop voltage.

Fig. 3. Electron distribution function at a radial location $r = 19.25$ cm versus parallel kinetic energy $E = m_e c^2 [n_\parallel/(n_\parallel^2 - 1)^{\frac{1}{2}} - 1]$ during LHRF ramp-up. The parameters are the same as in Fig. 2.

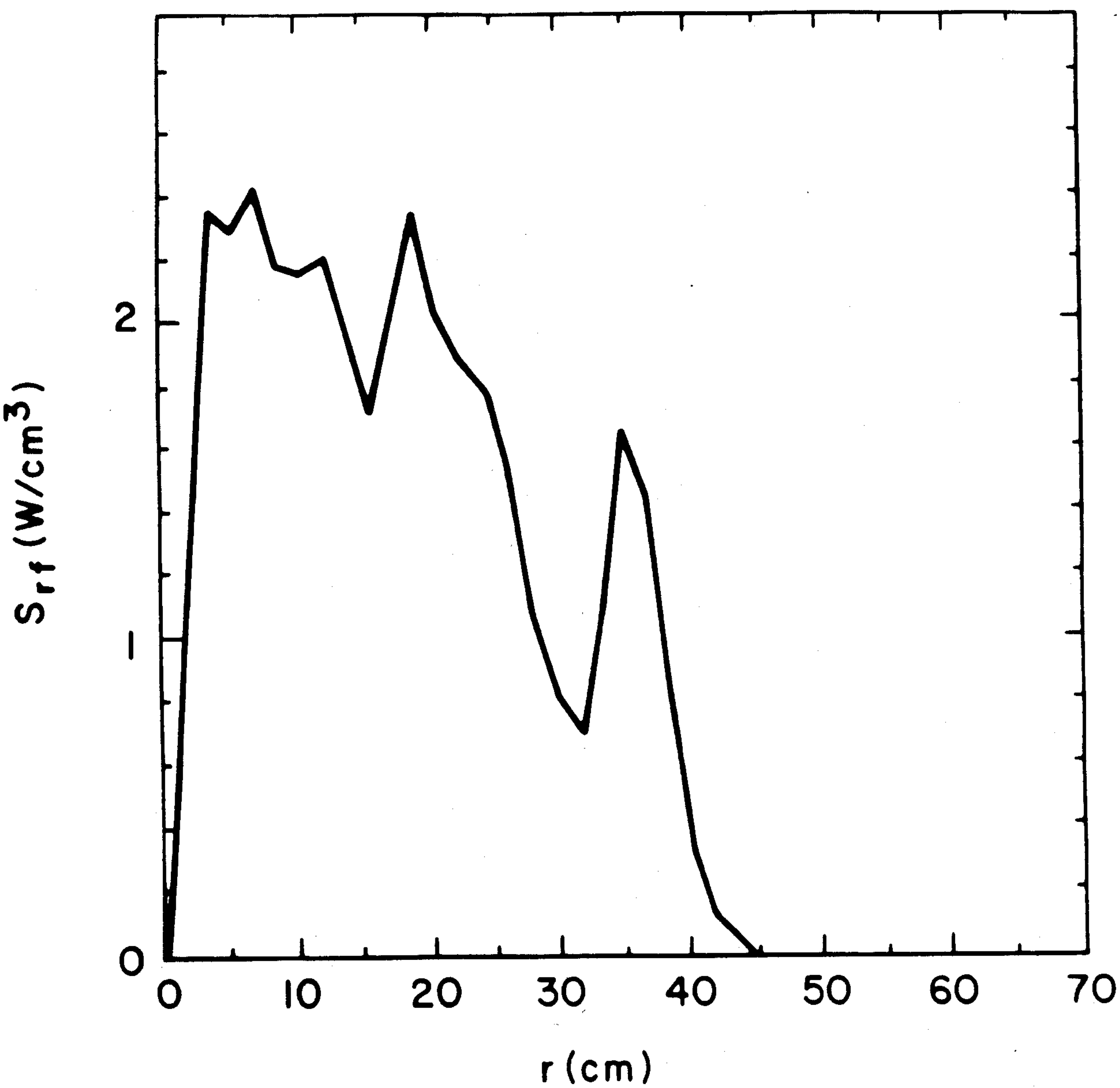

FIGURE 1(A)

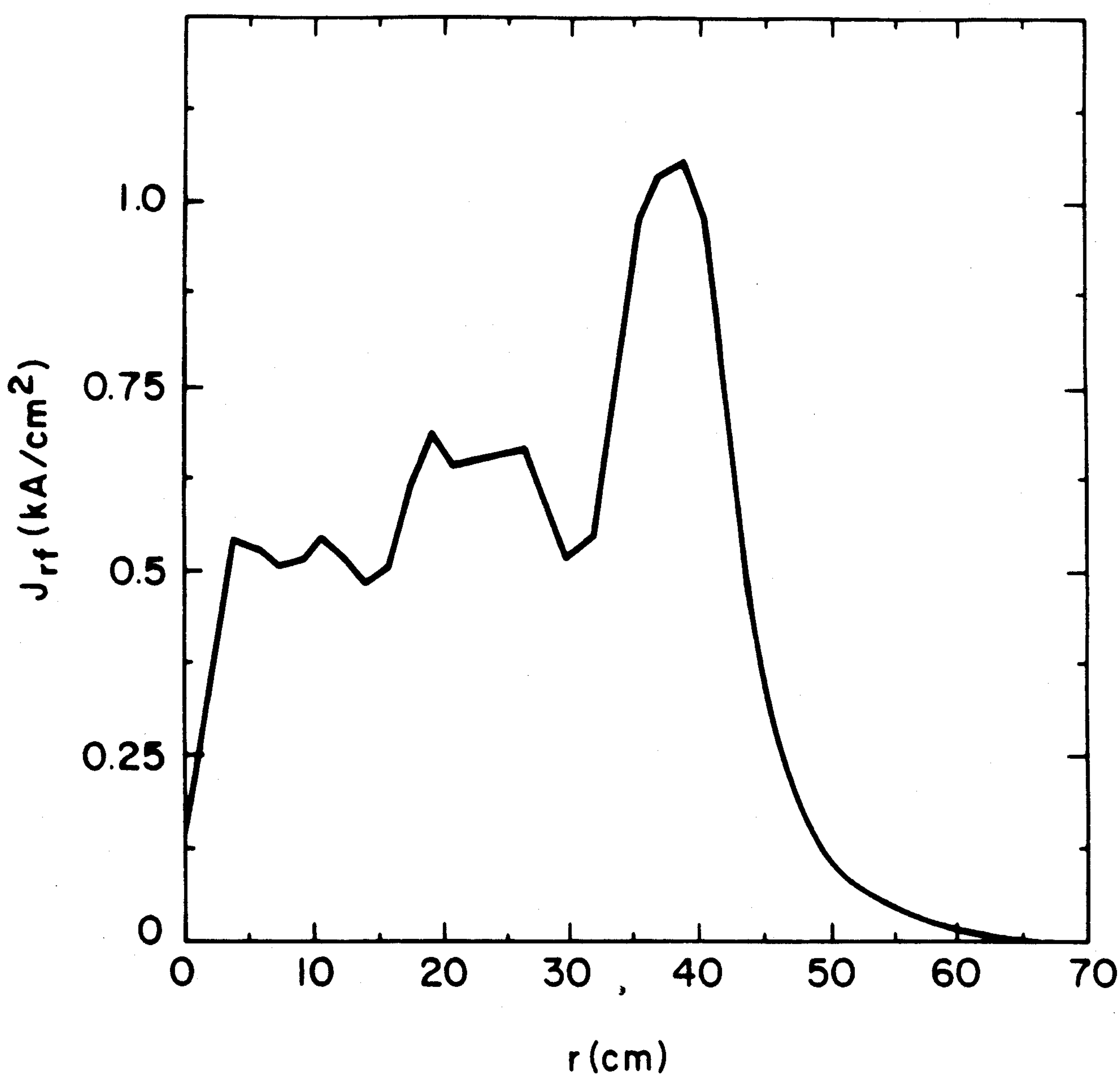

FIGURE 1(B)

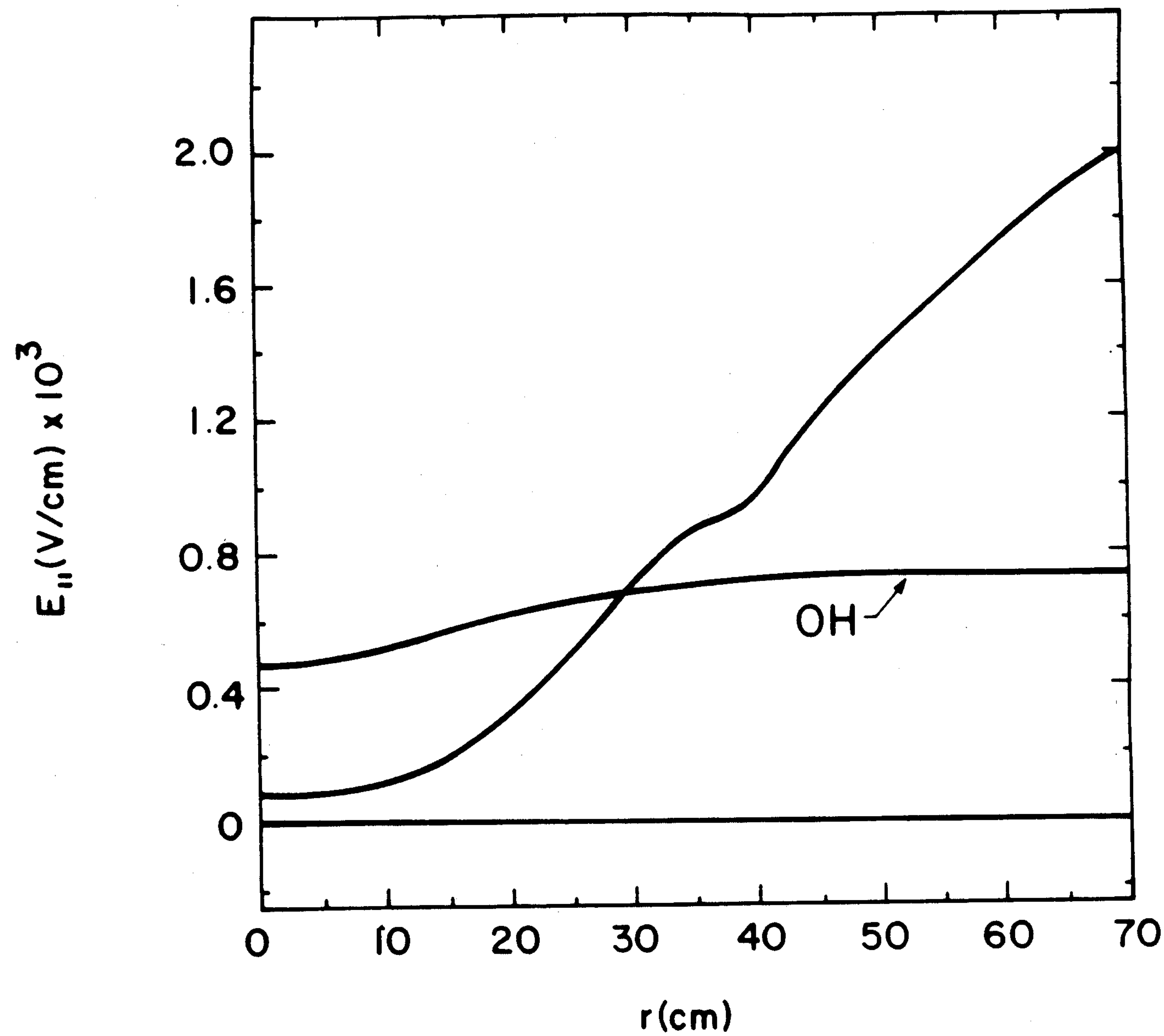

FIGURE 1(C)

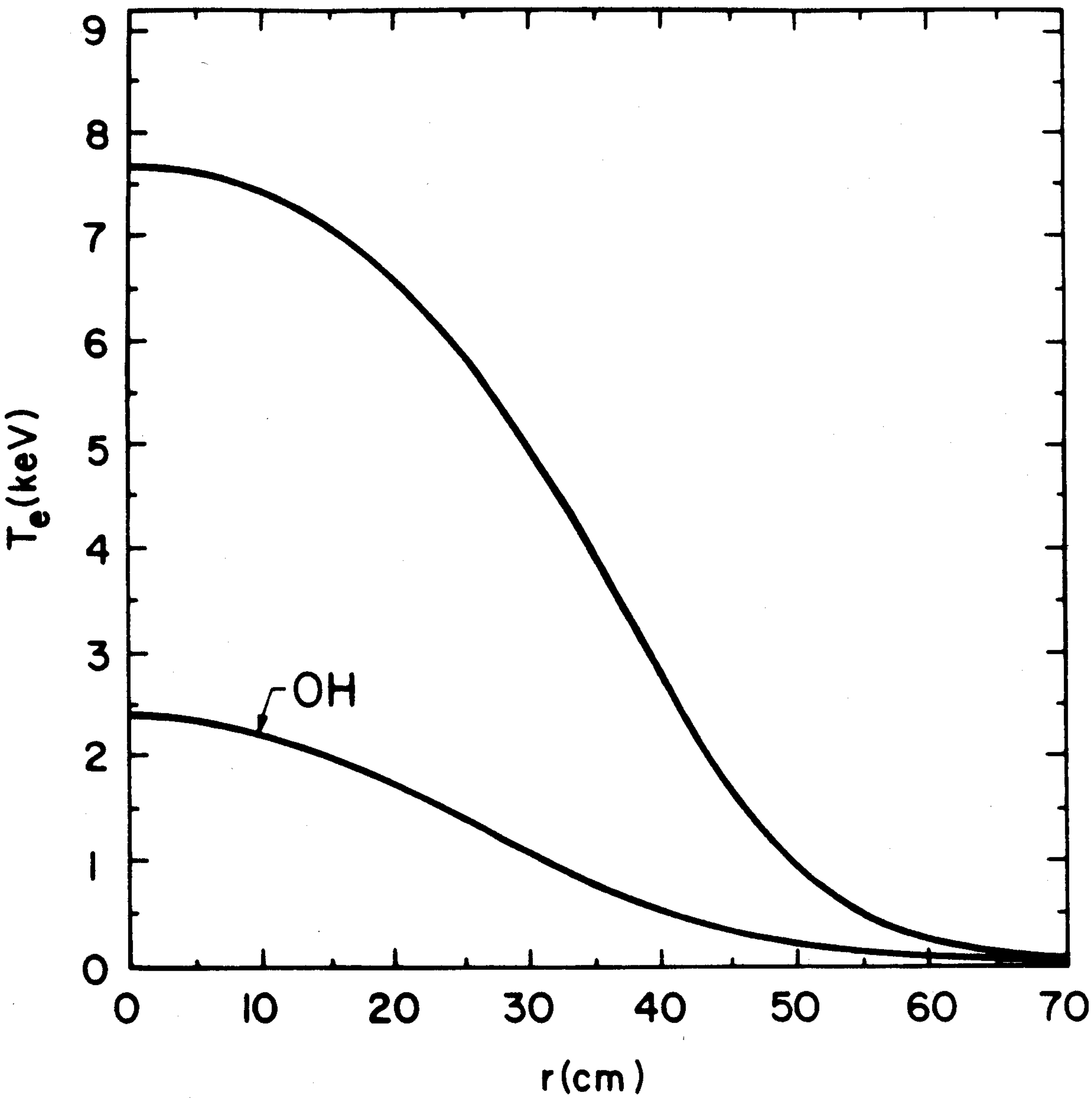

FIGURE 1(D)

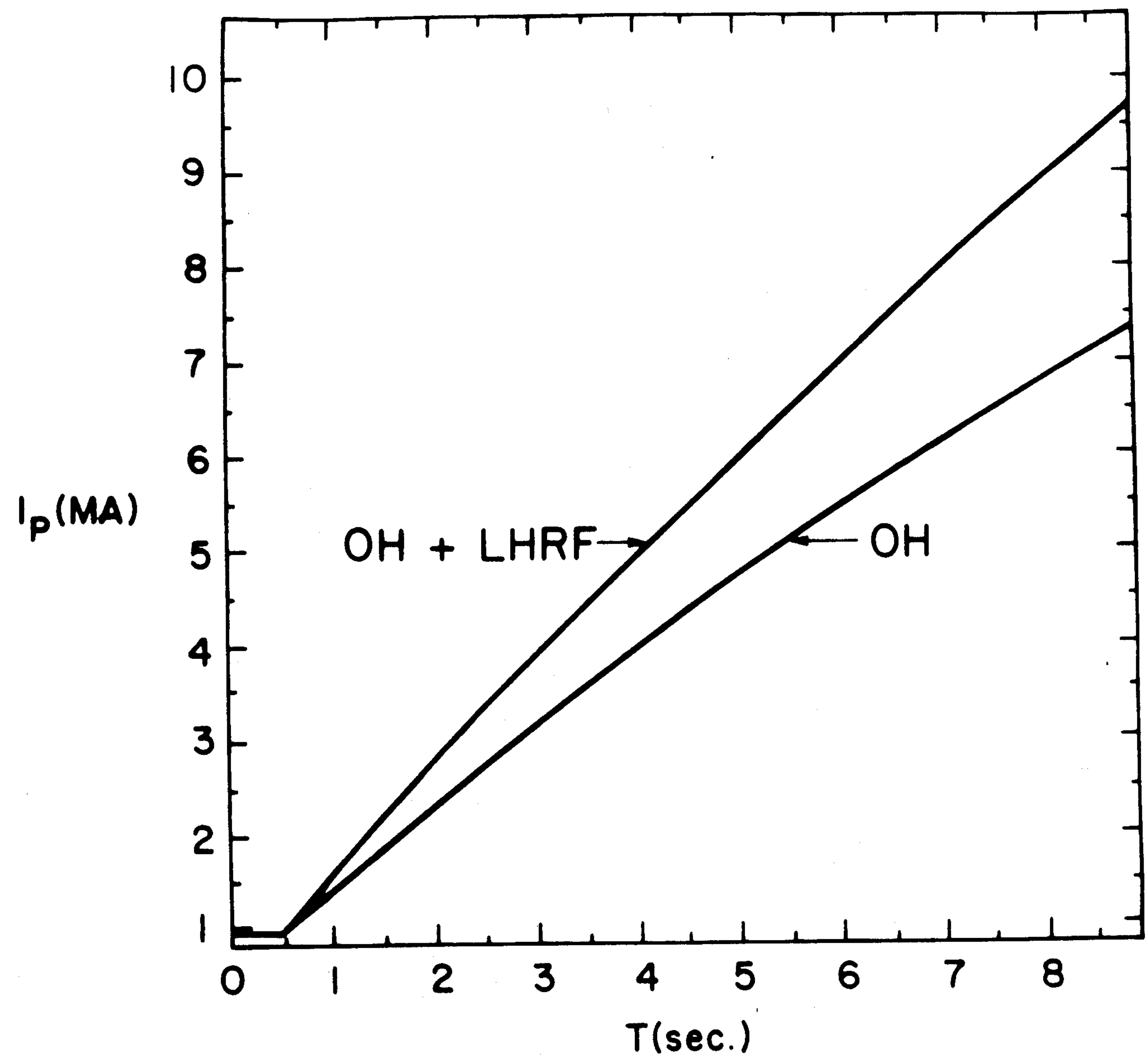

FIGURE 2(A)

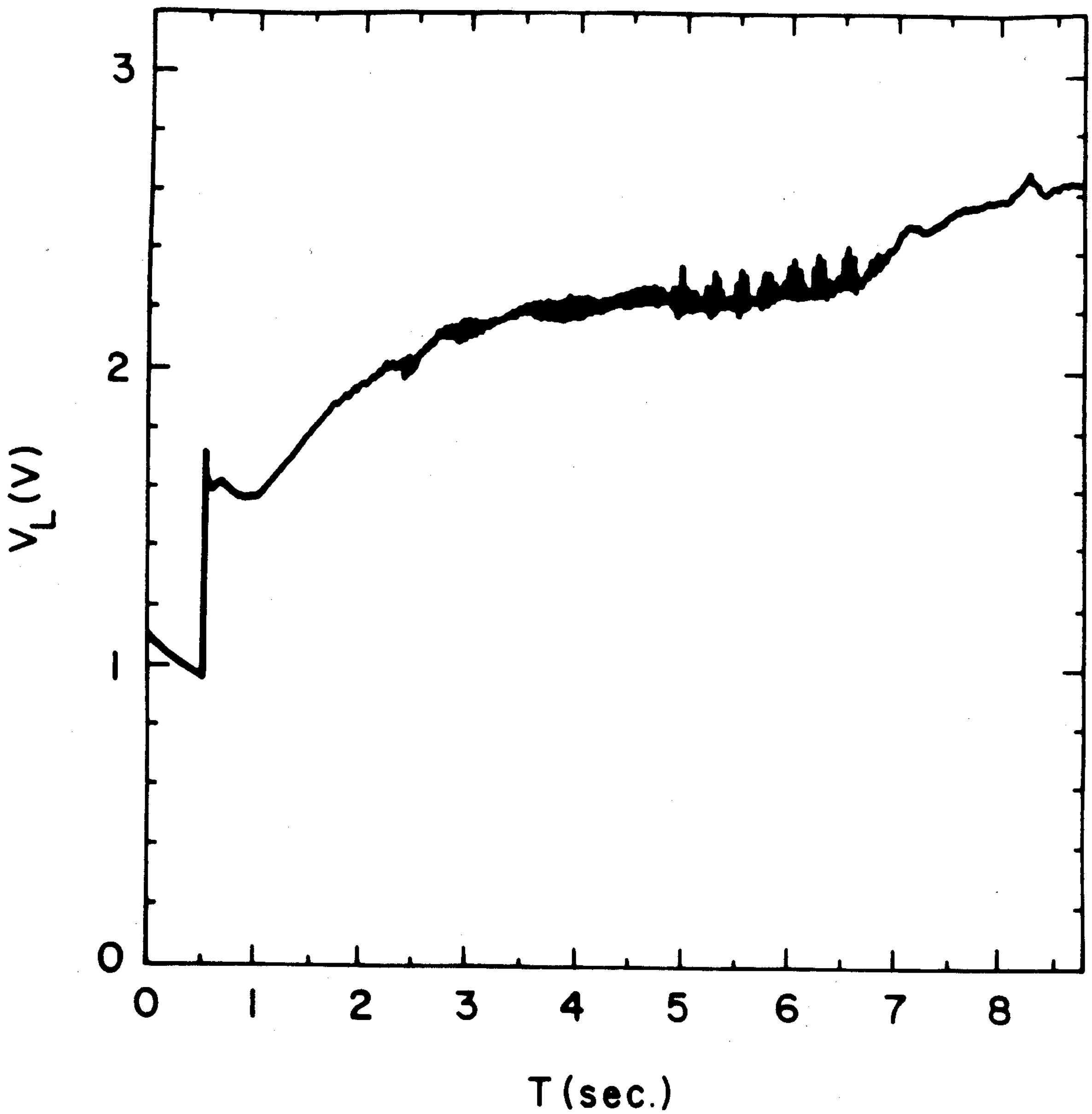

FIGURE 2(B)

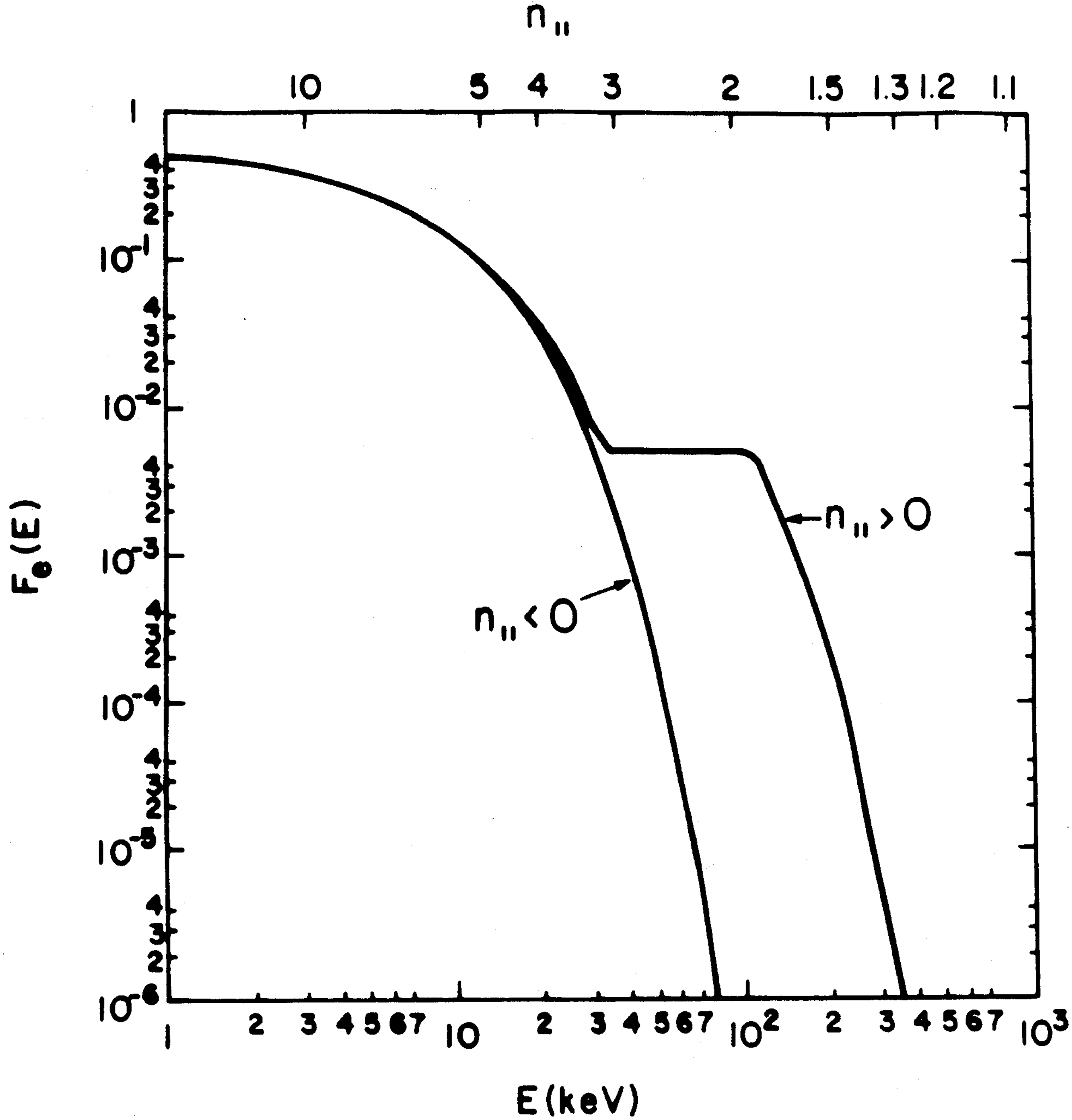
n∥
10
5
4
3
2
1.5
1.3
1.2
1.1
$F_e(E)$
10^{-1}
10^{-2}
10^{-3}
10^{-4}
10^{-5}
10^{-6}
$n_\parallel > 0$
$n_\parallel < 0$
1
10
10^2
10^3
E(keV)

FIGURE 3